ATLANTIS PRESS

Atlantis Highlights in Computer Sciences, volume 4

Proceedings of the 3rd International Conference on Integrated Intelligent Computing Communication & Security (ICIIC 2021)

Change Detection of LULC using Machine Learning

Geetha M[1,*], Asha Gowda Karegowda[2], Nandeesha R[3], Nagaraj B V[4]

[1]*Department of MCA, BIET, VTU, India*
[2]*Department of MCA, SIT, VTU, India*
[3]*Department of Civil Engineering, SIT, VTU, India*
[4]*Department of Management Studies, KIAMS, India*
[*]*Corresponding author. Email:bmgeethamallad@gmail.com*

ABSTRACT

This paper discusses detection of change in land usage in Davangere (Karnataka State, India) between the years 2016 and 2021. After the place has been declared as one of the smart cities identified by the Govt. of India in 2014 and subsequent to the international price crash for sugar, there were noticeable changes in land utilization in terms of urbanization and shift in traditional cropping pattern. The objective of this research work is to capture this change using remote sensing, the images from MSI Sentinel-2 were collected at two points of time and processed for LULC with the help of supervised machine learning classifiers such as Minimum Distance, Mahalanobis Distance and Maximum Likelihood to ascertain the accurate one. It was found that Maximum Likelihood classifier ensures highest accuracy of 95.2%. It was also found that during the study period, there was a significant change in the land use with respect to Built-up area and Area under cultivation of Paddy.

Keywords: *Accuracy, Change Detection, Classification, LULC, Sentinel 2.*

1. INTRODUCTION

Satellite images are widely used nowadays in varied fields like defence, oceanography, whether forecasts, precision agriculture and so on. One such application is to detect change in land usage from time to time using remote sensing techniques. Land use and Land cover (LULC) data collected for the given geographical area over a period of time indicate the change occurring during that span of time, which in turn helps regional administration to plan for development and resources. LULC assessment is made easy with the help of continuously evolving remote sensing techniques since last four decades. However continuous improvements in technology and satellite image processing techniques have paved way to discover and predict the ground realities as accurately as possible and hence an attempt has been made to find the change in land use pattern between two time points in this study.

2. RELATED WORK

Geographical Information System (GIS) and Remote Sensing serve array of applications in the fields of agriculture [1], environment [2], and ecological assessment [3]. Land use and land cover (LULC) is one such application that researchers and governments widely acknowledge in measuring the negative effects on ecology of the area and vegetation [4]-[7].

Mapping of LULC to monitor changes on the earth's surface using satellite image processing technologies has become one of indispensable tools across the globe since last two decades [8] although efforts were initiated during 1970s for application of different interpretation techniques [9]. LULC for a given geographical area is characterized by the geological structures, slopes, ecological conditions, elevations, along with technological, socio-economic changes taking place over a span of time [10]. Development of different LULC mapping techniques have demonstrated that measurement of land usage over a span of time has significant impact on the functioning of socio-economic and environmental systems with important trade-offs for biodiversity, ecological balance, food security, and peoples' socio-economic susceptibility and natural ecosystems [11].

Various (GIS) based satellite data sources with distinct capabilities and accuracy were developed by many nations across the globe. Landsat, LISS and Sentinel-2 are few of them [12].

The technique of Image classification is widely used in LULC studies [13]. Usually supervised classification technique is employed as a basic step.

The process of supervised classification starts by selecting sample locations of land cover types; this is known as training data/area. Then the algorithm uses the spectral signature of this training data to classify the image. Among supervised classification algorithms, Maximum likelihood, Mahalanobi's distance and Minimum-distance methods are the prominent ones. In maximum-likelihood classification algorithm, the unknown pixels are assigned to the specific class by using the contours probability around the training area. It is assumed that the statistical value for every class in every band is normally distributed and then the probability value that the pixel is appropriate to in a certain class is calculated. Every pixel is given to the class that has the highest probability [14].

The training data/plots are the small geographical areas identified by ground-truth approach to represent a particular study class [15]. Mahalanobi's distance algorithm assumes that the distribution of the bands possesses normal probability; variance and covariance are identified such that clusters that are highly varied, lead to similarly varied classes, and vice versa. The Minimum distance algorithm calculates the spectral distance between the given pixel vector and the mean vector for each signature. Thus this classification techniques extracts distance between any pair of pixels after defining training data.

Aicha Moumni and Abderrahman Lahroun (2021) [16] of Morocco conducted LULC studies to classify multiple crops using SVM, ANN and ML to obtain classification accuracy of 89% with Kappa coefficient of 0.85.

Shetty S (2019) [17] while analysing efficiency of classifiers for LULC using Random Forest, Support Vector Machine and Maximum likelihood classier applied on Google Earth Engine image found that random forest (RF) classifier to be the best with highest accuracy.

R. Hamad (2020) [18] in his research paper, An assessment of Artificial Neural Network (ANN), Support Vector Machine (SVM) and Decision Tree (DT) for land cover classification using sentinel-2A data found that ANN is the best classifier with 90% accuracy followed by SVM with 65% and DT with 60%.

Mahendra *et al.* (2019) [19] used Landsat-3 image to find the efficient classifiers among Mahalanobis distance, Minimum distance, Maximum likelihood and SVM and fond that SVM as the best classifier with 95.35% accuracy with Kappa of 0.94.

Land use and Land cover involves the process of identifying changes using temporal multispectral geo rectified images. Main objective of this research paper is to detect the changes in the geographical area of Davangere taluk between April 2016 and April 2021 using multispectral sentinel-2 data.

3. STUDY AREA

Davangere is one of the districts situated in central part of Karnataka with rich land and other resources. Large population of the district is dependent on agriculture and business. District has good agro climatic conditions with major crops being paddy, maize, coconut, areca, and sunflower besides other cereals and pulses. The study area is Davangere taluk with the total area of 958.23 sq. km. located between 14.4666ºN, 75.9242ºE.

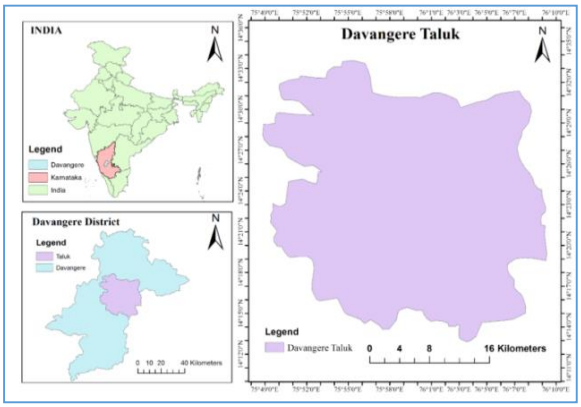

Figure 1 Location of Study Area

There have been two main reasons to investigate through this study. First among them was there are two fully integrated sugar manufacturing units in and around Davangere and hence there was a large base of sugarcane growing farmers since many years till 2015. In 2015, as there was a crash in international sugar prices and it lead to many sugar units in either not cutting the grown sugarcane at right time or not paying farmers in time. This made many farmers to shift from traditional sugar cultivation to paddy. The second reason was the announcement of government of India to develop Davangere as one of the smart cities in the 2014. This resulted in lot of revenue land conversions into residential plots and industrial areas. As a result of these two reasons there has been noticeable change in land utilization in the region. Thus the study intends to investigate the impact and estimate the change in land utilization between 2016 and 2021 for components such as water bodies, built-up area, area under paddy, fallow land and others [20-24].

4. DATA USED

Multispectral Sentinel-2 imagery has been used as the primary dataset for the classification of the study area. Sentinel-2 Images of 2016 and 2021 April were downloaded from Copernicus open access hub (https://scihub.copernicus.eu). Details are as in table-1. As Sentinel-2 images are optical in nature and only cloud free data that is available during the summer of

April 2016 and 2021 respectively are considered. As a result, the fallow land during the period of data collection has been very high which otherwise would be used to cultivate major crops like paddy, maize, sunflower, red gram etc.

Table 1. Details of Satellite data acquired

Satellite	Sensor	Resolution	Date of Acquisition
Sentinel-2	MSI	10m	April 22nd 2016
Sentinel-2	MSI	10m	April 1st 2021

5. METHODOLOGY

The satellite images so collected were processed using ERDAS Imagine and ArcGIS for classification of LULC. Processing of satellite image using ERDAS Imagine involves band stacking of multiple bands such as green, red and near infrared bands of 10m resolution, mosaicking, overlaying of study area and clipping of study area followed by supervised classification by generating training data using signature file. Study plots for paddy, horticultural crops, fallow land, waterbody, built-up, barren land and other land use classes were identified in the study area and the ground truth pertaining to their geographical coordinates were recorded as training data using android mobile app.

Further using training data various supervised classification algorithm such as Minimum Distance (KNN), Mahalanobis Distance and Maximum likelihood were used to classify the study area into various classes as Waterbody, Built-up, Paddy, Sugarcane, Fallow land, Barren and others to get the estimates of change in land utilization between 2016 and 2021.The sequential order of all these steps are presented in the flow diagram figure -2.

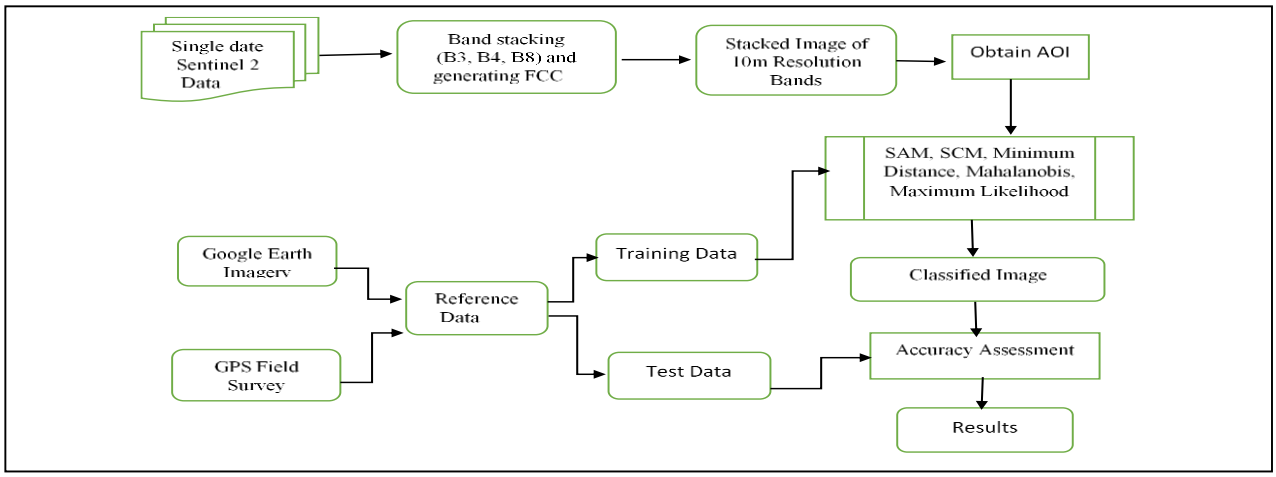

Figure 2 Steps of Image Processing using ERDAS Imagine

Characteristics of Classification Algorithms

The characteristics of different classification algorithms used in the study to evaluate their individual performance w.r.t. classification accuracy are as follows.

Minimum Distance Classification

It is the simplest form of supervised classification. This classifier calculates mean vector for each class and Euclidean distance from each pixel to the class mean vector and goes on assigning each pixel to the class to which it is closest thereby ensuring minimum distance and maximum similarity. Minimum distance is calculated as

$$d_k^2 = (X - \mu_k)^t (X - \mu_k) \quad (1)$$

Where d_k is the minimum distance; μ_k is the mean distance of kth class.

Maximum Likelihood Classification (MLC)

MLC uses the training data to conditionally calculate the likelihood of a pixel being in different classes on the available features such as of means and variances of the classes and variability of brightness for each class and assigns the pixel to the class having highest likelihood using Bayesian theory of probability hence considered to be one of the most widely used algorithms.

Assume that we have two classes ‘i’ and ‘j’. MLC assumes that the mean and variance for each class of each band are normally distributed. Each pixel is assigned to that class which has highest probability (maximum likelihood) [25-28]

Thus for a pixel at the point x, the pixel is assigned to class i if its probability of belonging to class i is

greater than that to class j. The pixel classification in MLC is based on minimum Euclidean distance from a class mean and direction sensitivity is based on covariance matrix. When sufficient training data is available with classes following normal probability characteristics, maximum likelihood classification is implemented by calculating the following discriminant function for each pixel

$$g_i(x) = \ln p(\omega_i) - \frac{1}{2}\ln|Ci| - \frac{1}{2}(x - m_i)^t C_i^{-1}(x - m_i) \quad (2)$$

Where g_i (x) = discriminant function of a pixel in i^{th} class

P(ωi) = Probability that class ω_i occurs in the image and is same for all classes
|Ci | = Determinant of covariance matrix of the data in ω_i^{th} class
x = n-dimensional data (n is the number of bands)
mi = Mean vector and ***t*** = transpose of the base

Mahalanobi's Distance Classification

Mahalanobis distance classification algorithm assigns a class based on covariance measured between classes and hence considered to be more accurate when compared to Euclidean distance. The Mahalanobis distance is calculated using

$$M_h^2 = (x - m_i)^t C_i^{-1}(x - m_i) \quad (3)$$

Where M_h = Mahalanobis distance.

Overall accuracy and corresponding KHAT value (Kappa Coefficient) of classifications made using different approaches was calculated using the obtained confusion matrix with the help of following relations [29-34].

$$\text{Overall Accuracy} = \frac{Correctly\ classified\ pixels}{Total\ Number\ of\ pixels} \quad (4)$$

$$Kappa\ Coefficient,$$

$$k = \frac{Observed\ Accuracy - Chance\ agreement}{1 - chance\ agreement} \quad (5)$$

$$\text{i.e., } \boldsymbol{k} = \frac{N\sum_{i=1}^{r} x_{ii} - \sum_{i=1}^{r}(x_{i+}.x_{+i})}{N^2 - \sum_{i=1}^{r}(x_{i+}.x_{+i})} \quad (6)$$

Where,

r = number of rows in error matrix
$\boldsymbol{x_{ii}}$ = diagonal observations in error matrix
$\boldsymbol{x_{i+}}$ = total number of observations of ith row;
$\boldsymbol{x_{+i}}$ = total number of observations of ith column
and ***N*** = grand total of all observations in error matrix.

Various stages of satellite image processing using ERDAS Imagine are as presented in figure-3.

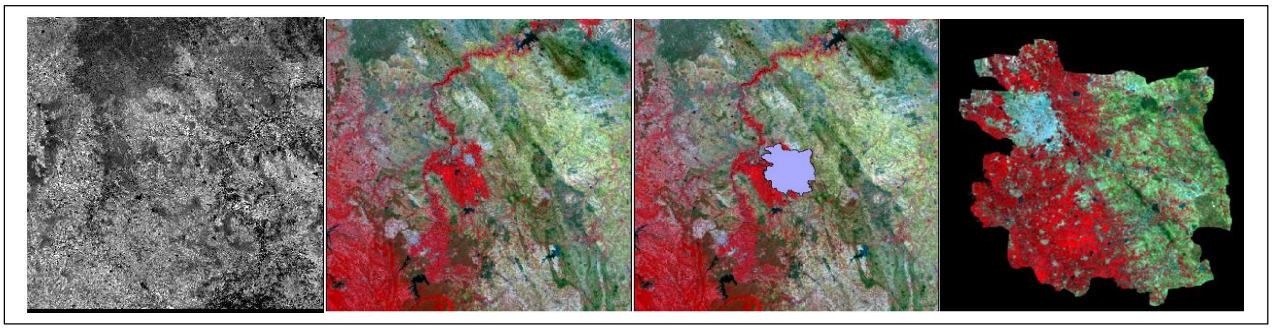

(a) **(b)** **(c)** **(d)**

Figure 3 Stages of image processing viz., Single band (a), Band stacking and mosaicking (b) overlaying (c) and Clipping (d)

6. RESULTS AND DISCUSSION

Sentinel 2 images for the years 2016 and 2021 were classified into seven classes i.e. paddy, horticultural crops, fallow land, waterbody, built-up, barren land and other land` use to detect the intended change. Each class will have its own specific spectral signature and hence distinct reflectance. The acquired image contains thirteen spectral bands, off which three spectral bands of 10 m resolution viz., green (560 nm), red (665 nm) and near infrared (842 nm) were chosen to obtain composite layer. The classified maps for seven identified classes for the years 2016 and 2021were obtained using minimum distance, Mahalanobi's distance and maximum likelihood classifiers along with the corresponding accuracy assessment matrices. One such map using maximum likelihood classifier has given overall accuracy of 95.5% and 92.8% (for 2016 and 2021 respectively, which is highest among three classifiers used in the study: Ref. Table-4) is shown in figure-4 and figure-5 respectively.

The classified images of 2016 and 2021 show the notable separation between the classes. The classification results show the accuracy of 71.8% and 74.5% with KHAT of 0.66 and 0.67 (for 2016 and 2021 respectively) using minimum distance classifier. Classification accuracy of 93.8% and 90.7% with KHAT of 0.92 and 0.87 was obtained by Mahalanobi's distance classifier, whereas accuracy of 95.5% and 92.8% with KHAT of 0.94 and 0.9.

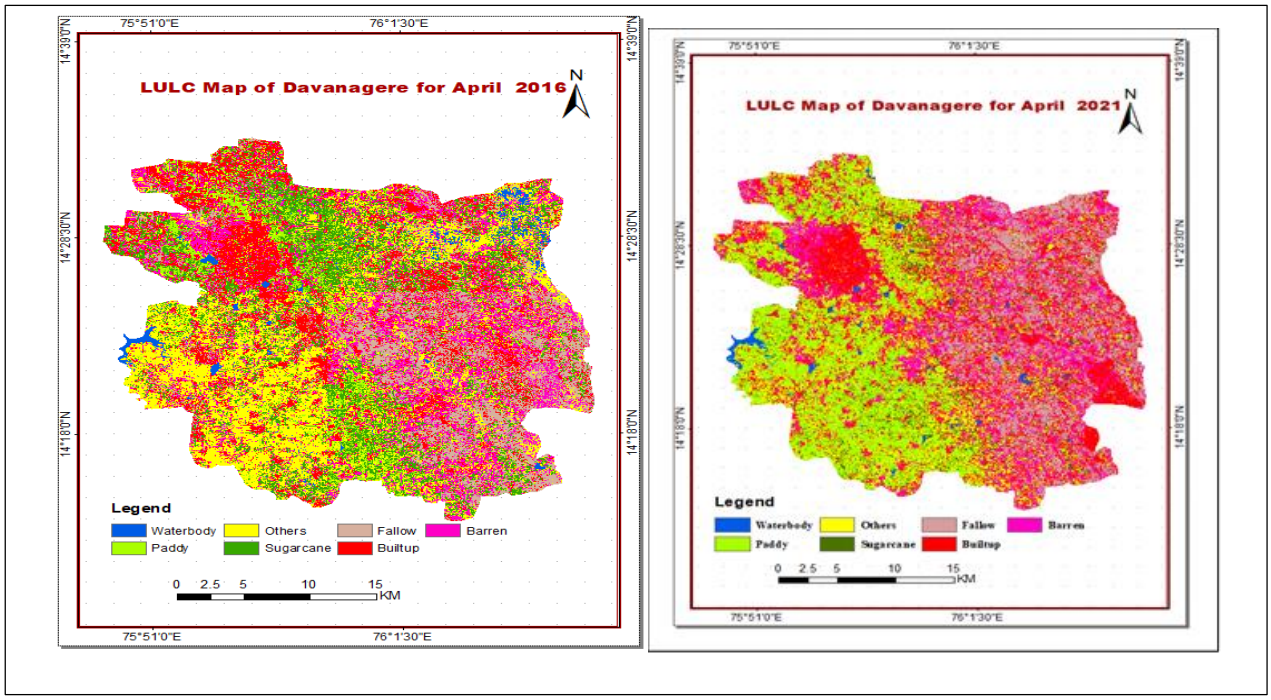

Figure 4 LULC of study area in April 2016

Figure 5 LULC of study area in April 2021

To ascertain best possible classification accuracy, three algorithms such as minimum distance, Mahalanobi's distance and Maximum likelihood were used and overall accuracy and Kappa coefficient for each of the classification were separately calculated. These metrics derived from respective accuracy assessment matrices are as shown in table-2 through table-5.

Table 2. User's Accuracy (UA) and Producer's Accuracy (PA) for classifications under study in 2016

Classifiers	Waterbody		Barren		Horticulture		Fallow		Paddy		Built up		Others	
	UA	PA	UA	PA	UA	PA	UA	PA	UA	PA	UA	PA	UA	PA
Minimum Distance	92.3	94.4	78.7	81.3	89.7	66	45.6	47	79.6	93.4	25.8	48.8	76	51.6
Mahalanobis Distance	99.3	98.6	83.4	87.2	95.8	82.1	93.3	65.2	97.3	89.7	90.4	88.2	94.8	99.2
Maximum Likelihood	99.4	98.6	97.8	92.6	92.5	97.2	86.9	95	96.7	93.4	91.5	93.1	97.8	95.8

Table 3. User's Accuracy (UA) and Producer's Accuracy (PA) for classifications under study in 2021

Classifiers	Waterbody		Barren		Horticulture		Fallow		Paddy		Built up		Others	
	UA	PA	UA	PA	UA	PA	UA	PA	UA	PA	UA	PA	UA	PA
Minimum Distance	95.2	99.9	53.6	72.9	60.9	77.3	51.1	52.6	96.4	84	94.2	65.1	71	88.3
Mahalanobis Distance	99.9	99.8	63.2	54	59.6	89.9	95.2	86.2	98.2	86.7	93.5	96.6	75.3	95.7
Maximum Likelihood	99.8	99.8	79.9	93.7	69.8	84.2	90.7	93.5	96.9	91.5	99	95.3	78	95.8

Table 4. Comparative Overall accuracy (%) in classification

Classification Algorithm	Overall Accuracy (%)	
	2016	2021
Minimum Distance	71.8	74.5
Mahalanobi's Distance	93.8	90.7
Maximum Likelihood	95.5	92.8

Table 5. Comparative Kappa coefficient for classification done

Classification Algorithm	KHAT (Kappa Coefficient)	
	2016	2021
Minimum Distance	0.660	0.672
Mahalanobis Distance	0.923	0.876
Maximum Likelihood	0.944	0.900

Table-4 and Table-5 show the statistics of the classification results for Minimum Distance, Mahalanobis Distance and Maximum Likelihood Classifiers. The results show that the Maximum Likelihood classifier classifies the image with best overall accuracy of 95.5% and 92.8% with KHAT value of 0.944 and 0.900 respectively.

Classification done for different land utilization dimensions for two study years were obtained based on the best classifier (Maximum likelihood) and noted as in Table-6.

Table 6. LULC of study area and their changes (Area in Ha.)

Class Name	2016	2021	Difference	Change %
Waterbody	1787.1	1084.2	-702.87	-39.3*
Built up	8076.7	8478.2	401.44	4.7
Paddy	2200.1	2820.2	620.08	22.0
Sugarcane	2580	1646.1	-933.84	-36.2
Fallow (Agri.+Non Agri.)**	54675	53680	-995	-1.8
Barren	9630	9546	-84	-0.9
Others	16878.4	18571.8	1693.36	9.1
Total Area [Hectares (Ha.)]	95827.5	95826.7		

Notes: * Decline in waterbody to the extent of 39.3% in 2021 as compared to 2016 was due to the reason that one of the largest lakes of Davangere i.e., Kundawada lake is drained in 2021 to increase the depth to build higher water holding capacity.

** Fallow land comprises of larger part of agricultural (Over 20000 Ha of land is used for paddy alone during monsoon and winter) is used for and non-agricultural fallow land as the assessment is being done in summers of 2016 and 2021 when cultivation is carried out only at irrigated/lands having adequate water sources in the study area.

As it can be noticed from table-3, there is an increase in land utilization for built-up areas by 4.7% and for area under cultivation of paddy by 22% between 2016 and 2021.

The increase in built-up area from 2016 to 2021 can be attributed to the increasing urbanization during the study period as a result of Davangere being one of the developing smart cities and the tendency of people from far off places of the state choosing the place as their real estate investment destination.

The increase of whopping 22% area under cultivation of paddy was due to the shift of traditional farmers growing sugarcane for many years in the past towards cultivation of paddy as there was a price crash for sugar in international market in 2015, which effected local sugar processing units to delayed cutting of sugarcane from contract farmers which lead to delayed payments. As a result, large number of farmers growing sugarcane shifted to paddy cultivation and plantation of coconut and areca from 2016 and onwards. This is even indicated in increase of 9.1% for others (which include horticulture crops like coconut and areca).

There is a decline in total land utilization for cultivation of commercial crop sugarcane to the extent of 36.2%. It was again due to the shift of sugarcane farmers to paddy cultivation during the study period.

Table 7. Comparative Assessment of Accuracy

Author(Year)	Classifier	Accuracy (%)	Kappa
R. Hamad (2020)	ANN*	90	0.86
Aicha Moumni(2021)	SVM**	89	0.85
Proposed Study (2021)	MLC	92.8	0.9

*** Artificial** Neural **Network;**

**** Support** Vector **Machine**

7. CONCLUSION

Based on the results evaluated, the Maximum Likelihood Classifier (MLC) is found to be the efficient classifier with best overall accuracy and Kappa coefficient. However, the results obtained using Mahalanobi's Distance are better than that of Minimum Distance and they suit well for some classes of specific interest only. Thus as evident from the study, one can make out the fact that whenever there are leap changes in administrative policies of the government, it leads to changes in economic variables like land prices (in the context of present study), trends and tendencies of people thereby initiating change in land utilization pattern from time to time. The study shows increase of 4.7% land utilization for built-up area; increase of 9.1% land utilization under others class, increase of 22% land for paddy cultivation and 36.2% decrease in cultivation of sugarcane during the study period between 2016 1nd 2021.

Assessment of LULC at times therefore serves as necessary tool for the government authorities and decision makers in devising better future infrastructural policies, agricultural policies and city planning apart from knowing the rate of change from time to time. With regards to accuracy of different classification algorithms (classifiers) used in the present study, Maximum Likelihood algorithm stand out to be the best estimator with overall accuracy of 95.5% and 92.8% with Kappa coefficient of 0.944 and 0.9 respectively.

ACKNOWLEDGMENT

We thankfully acknowledge the invaluable support extended by institutions like KSRSAC, GKVK and ISRO Bengaluru, KVK, Dept. of Agriculture, DSO and ZP offices of Davangere in developing this research work.

REFERENCES

[1] A. G. O. Yeh and X. Li, Principal component analysis of stacked multi-temporal images for the monitoring of rapid urban expansion in the Pearl River, International Journal of Remote Sensing, 1998,Vol. 19, No. 8, pp. 1501–1518.

[2] T. Fung and E. Ledrew, Application of principal components analysis to change detection, Photogrammetric Engineering & Remote Sensing, 1987, Vol. 53, No. 12, pp. 1649–1658.

[3] H. Long, X. Wu, W. Wang, and G. Dong, Analysis of urban rural land-use change during 1995-2006 and its policy dimensional driving forces in Chongqing, China, Sensors, 2008, Vol. 8, no. 2, pp. 681–699.

[4] M. El-Raey, Y. Fouda, and P. Gal, GIS for environmental assessment of the impacts of urban encroachment on Rosetta region, Egypt , Environmental Monitoring and Assessment, 2000,Vol. 60, No. 2, pp. 217–233.

[5] S. Martinuzzi, W. A. Gould, and O. M. R. Gonz´alez, Land development, land use, and urban sprawl in Puerto Rico integrating remote sensing and population census data, Landscape and Urban Planning, 2007,Vol. 79, No. 3-4, pp. 288–297.

[6] H. S. Sudhira, T. V. Ramachandra, and K. S. Jagadish, Urban sprawl: metrics, dynamics and modelling using GIS, International Journal of Applied Earth Observation and Geoformation, 2004, Vol. 5, No. 1, pp. 29–39.

[7] S. Hathout, The use of GIS for monitoring and predicting urban growth in East and West St Paul, Winnipeg, Manitoba, Canada, Journal of Environmental Management, 2002,Vol. 66, No. 3, pp. 229–238.

[8] Sadat, H., Adamowski, J., Bonnell, R., Sharifi, F, Namdar, M., Ale-Ebrahim, S. Land use and land cover classification over a large area in Iran based on single date analysis of satellite imagery, ISPRS J. Photogrammetry Remote Sens, 2011,Vol 66, pp.608–619.

[9] Zhang, P., L, Z., Shi, W, Local spectrum-trend similarity approach for detecting land-cover change by usingspot-5 satellite images, IEEE Geosci. Remote Sens. Lett. 2014, Vol.11, 7pp.38–742.

[10] Rai, S.C., Sharma, E., Sundriyal, R.C., Conservation in the Sikkim Himalaya: traditional knowledge and land-use of the Mamlay watershed, Environ. Conserv. 1994, Vol.21, No.1, pp.30–34.

[11] Dimyati, M.U.H., Mizuno, K., Kobayashi, S, Kitamura, T, An analysis of land use/cover change

in Indonesia, Int. J. Remote Sens. 1996, Vol.17, No.5, pp.931–944.

[12]Barnsley, M.J, Moller-Jensen, L, Barr, S.L, Inferring urban land use by spatial and structural pattern recognition, Remote Sens. 2001, Urban Anal., pp.115–144.

[13] H. Saadat, J. Adamowski, R. Bonnell, F. Sharifi, M. Namdar, S. Ale-Ebrahim, Land Use and Land Cover Classification over A Large Area in Iran Based on Single Date Analysis of Satellite Imagery, ISPRS Journal of Photogrammetry and Remote Sensing, 2011,Vol.66, pp.608–619.

[14] B.R. Deilmai, B. Bin Ahmad, H. Zabihi, Comparison of two Classification methods (MLC and SVM) to extract land use and land cover in Johor Malaysia, In IOP Conference Series: Earth and Environmental Science, 2014,Vol. 20, pp.1-6.

[15] Purkis, S.J., Klemas, V.V, Remote Sensing and Global Environmental Change, 2011, John Wiley & Sons.

[16] Aicha Moumni and Abderrahman Lahroun, Machine Learning-Based Classification for Crop-Type Mapping Using the Fusion of High-Resolution Satellite Imagery in a Semiarid Area, 2021, Hindawi Scienifica, pp 1-20.

[17] Shetty S. Analysis of machine learning classifiers for LULC classification on google earth engine, Thesis submitted to the Faculty of Geo-Information Science and Earth Observation of the University of Twente, 2019.

[18] R. Hamad , An assessment of artificial neural networks, support vector machines and decision trees for land cover classification using sentinel-2A data, Sciences 8 (6) 2020 pp. 459–464.

[19] Mahendra H N et.al. Performance Analysis of Different Classifier for Remote Sensing Application, International Journal of Engineering and Advanced Technology 2019, Vol.9 Issue 1, pp. 7153-7158.

[20] Remote Sensing and Image Interpretation by Lillesand, Kiefer and Chipman, Wiley Publications, 6e, 2018, pp 582 – 591.

[21] Prabu, S., Balamurugan Velan, F. V. Jayasudha, P. Visu, and K. Janarthanan. "Mobile technologies for contact tracing and prevention of COVID-19 positive cases: a cross-sectional study." International Journal of Pervasive Computing and Communications (2020).

[22] Bhuvaneswary, N., S. Prabu, S. Karthikeyan, R. Kathirvel, and T. Saraswathi. "Low Power Reversible Parallel and Serial Binary Adder/Subtractor." Further Advances in Internet of Things in Biomedical and Cyber Physical Systems (2021): 151.

[23] Hu, Liwen, Ngoc-Tu Nguyen, Wenjin Tao, Ming C. Leu, Xiaoqing Frank Liu, Md Rakib Shahriar, and SM Nahian Al Sunny. "Modeling of cloud-based digital twins for smart manufacturing with MT connect." Procedia manufacturing 26 (2018): 1193-1203.

[24] Nguyen, Tu N., Bing-Hong Liu, Nam P. Nguyen, and Jung-Te Chou. "Cyber security of smart grid: attacks and defenses." In ICC 2020-2020 IEEE International Conference on Communications (ICC), pp. 1-6. IEEE, 2020.

[25] Naeem, Muhammad Ali, Tu N. Nguyen, Rashid Ali, Korhan Cengiz, Yahui Meng, and Tahir Khurshaid. "Hybrid Cache Management in IoT-based Named Data Networking." IEEE Internet of Things Journal (2021).

[26] Puttamadappa, C., and B. D. Parameshachari. "Demand side management of small scale loads in a smart grid using glow-worm swarm optimization technique." Microprocessors and Microsystems 71 (2019): 102886.

[27] Rajendran, Ganesh B., Uma M. Kumarasamy, Chiara Zarro, Parameshachari B. Divakarachari, and Silvia L. Ullo. "Land-use and land-cover classification using a human group-based particle swarm optimization algorithm with an LSTM Classifier on hybrid pre-processing remote-sensing images." Remote Sensing 12, no. 24 (2020): 4135.

[28] Rajendrakumar, Shiny, and V. K. Parvati. "Automation of irrigation system through embedded computing technology." In Proceedings of the 3rd International Conference on Cryptography, Security and Privacy, pp. 289-293. 2019.

[29] Z. Guo, L. Tang, T. Guo, K. Yu, M. Alazab, A. Shalaginov, “Deep Graph Neural Network-based Spammer Detection Under the Perspective of Heterogeneous Cyberspace”, Future Generation Computer Systems, https://doi.org/10.1016/j.future.2020.11.028.

[30] N. Shi, L. Tan, W. Li, X. Qi, K. Yu, “A Blockchain-Empowered AAA Scheme in the Large-Scale HetNet”, Digital Communications and Networks, https://doi.org/10.1016/j.dcan.2020.10.002.

[31] L. Tan, H. Xiao, K. Yu, M. Aloqaily, Y. Jararweh, "A Blockchain-empowered Crowdsourcing System for 5G-enabled Smart Cities", Computer Standards & Interfaces, https://doi.org/10.1016/j.csi.2021.103517

[32] K. Yu, L. Tan, X. Shang, J. Huang, G. Srivastava and P. Chatterjee, "Efficient and Privacy-Preserving Medical Research Support Platform Against COVID-19: A Blockchain-Based Approach", IEEE Consumer Electronics Magazine, doi: 10.1109/MCE.2020.3035520.

[33] Z. Guo, K. Yu, Y. Li, G. Srivastava, and J. C. -W. Lin, "Deep Learning-Embedded Social Internet of Things for Ambiguity-Aware Social Recommendations", IEEE Transactions on Network Science and Engineering, doi: 10.1109/TNSE.2021.3049262.

[34] Z. Guo, A. K. Bashir, K. Yu, J. C. Lin, Y. Shen, "Graph Embedding-based Intelligent Industrial Decision for Complex Sewage Treatment Processes", International Journal of Intelligent Systems，2021, doi: 10.1002/int.22540